Available online at www.sciencedirect.com

ScienceDirect

Procedia Engineering 109 (2015) 346 – 355

Procedia Engineering

www.elsevier.com/locate/procedia

XXIII Italian Group of Fracture Meeting, IGFXXIII

# Evaluation of the relative plastic work factor during the fatigue test

A. Risitano, G. Fargione*, F. Giudice, G. Patanè

*Department of Industrial Engineering, University of Catania, Viale Andrea Doria 6, 95125 Catania, Italia*

**Abstract**

The evaluation of the temperature rising during a fatigue test is extremely important to define the energy method to be used. In order to define the best load program and the more appropriate test frequency, it is necessary to estimate the surface temperature of the material, in particular when it's needed to arrange some tests on mechanical components. With regards to the energetic approach to the study of fatigue phenomena, in the past the internal damping factor was considered an important parameter to define the fatigue quality of the material used for the mechanical application. In the present paper the role of another important work parameter is highlighted, when linked to the plastic strain caused by the high number of fatigue tests. An approach to the detection of first microplasticization and crack beginning is also proposed, with a model for the estimation of the crack propagation during the last cycles of fatigue test.



Peer-review under responsibility of the Gruppo Italiano Frattura (IGF)

*Keywords:* Fatigue; Energy method; Damping; Crack propagation; Termography

## 1. Introduction

The present study is focused on the energy release in the materials subjected to the loads application in fatigue tests. Since the early '50s Foppel and his school has noticed and studied the phenomenon of the temperature rising in the specimens if stressed to fatigue [1]. He tied up the variation of the temperature with the internal damping of the materials. In 1934 Taylor et al. studied the latent energy remaining in the metal after the cold working [2]. In assessing the fatigue limit by increasing the load during the test, Dengel and Harrig [3] noticed and measured the temperature variations. With the introduction of the high-precision sensors and, in particular of the thermal infrared sensing techniques, the phenomenon of the heat release of the materials under stress has become more interesting for the researchers, because they noticed that it could become an indicative parameter for the study of the materials

* Corresponding author. Tel.: +39-095-7382419; fax: +39-095- 337994.
*E-mail address:* gfargion@dii.unict.it


Peer-review under responsibility of the Gruppo Italiano Frattura (IGF)
doi:10.1016/j.proeng.2015.06.242

fatigue [4]. Since 1980 the number of scholars interested in this field of research has significantly grown, and fast methods to determine the fatigue limit have been proposed. Beginning from 1984 Geraci, Risitano et al. [5-13] proposed a new method based on the following observation on the material behavior: if the stress values were lower than the fatigue limit, the temperature didn't rise on the surface of the specimen. Some other methods based on the same observation have been later proposed and implemented by other researchers [14-23]. In all the cases, it has been verified that for the loads lower than the fatigue limit, the heat produced by the internal elastic damping or stored as deformation energy, generates minimal heat increments. It is not the same if on the material occurs irreversible phenomena with plastic deformations. The study of the heat released by the metallic materials stressed over the fatigue limit, in fact, defined the typical diagram of the surface temperature reported in Fig.1. It can be divided into three different phases [5-13]:

- Phase A. A gradual change in the structure of the material occurs, with continuous dislocations and structural rearrangements.
- Phase B. It is characterized by a quasi-equilibrium thermal state and the increment of temperature (as to the ambient temperature) on the surface of the specimen is constant (ΔT=constant).
- Phase C. It concerns the growth of the crack and it is characterized by a sudden increase in temperature. During this phase the length of the crack increases up to the break for failure of the specimen or of the component. The third phase is characterized by a number of cycles limited if compared to that of the second phase.

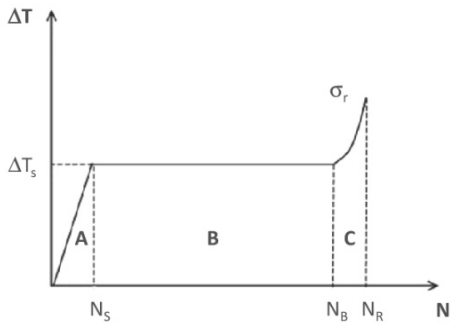


Fig. 1. Trend of the temperature increment with loads over the fatigue limits.

The diagram of Fig. 1 is characterized by a value of the applied stress which exceeds the fatigue limit. During the B phase, the energy dissipation that generates heat is due to both phenomena of internal elastic damping and of microplasticity. Maquin F. et a. in [24] proposed analytical models to separate the heat sources.

In this work fatigue tests have been performed on some specimens of X5CrNi1810 steel, recording continually their surface temperature due to the applied "stepped" stresses. The plastic deformation on varying the strain has been evaluated. For each of the examined specimens they have been detected the beginning of the crack formation (start of phase C), and the rise of temperature which increases the length of the crack until the complete breakage.

## 2. Theoretical modeling based on the energy balance

The theoretical model that could be referred to for the study of the energy balance in fatigue tests [25-27] is simple if the phenomenon is reduced to the case of a flat specimen with a constant temperature (phase B in the diagram of Fig. 1). The work supplied from the outside per volume unit and per cycle is equal to the integral of the product of the components of the main stresses for the respective elementary components of deformation. In the case of axial stress, it is:

$$W = \oint \sigma \, d\varepsilon \tag{1}$$

where $W$ is the energy per volume unit and per cycle delivered to the specimen from the outside (supplied energy), $\sigma$ is the axial stress (main component), $\varepsilon$ is the elementary strain according to the main direction. If $Q$ is the energy transformed into heat, and $\Delta U$ is the part which causes the variation of the internal energy, the energy balance is:

$$W = Q + \Delta U \tag{2}$$

The internal variation of energy $\Delta U$ is composed in its turn by the part which causes the raise of the specimen temperature (the analyzed volume) and by the part which accrues as fatigue, cycle by cycle, until reaching the limit value $E_l$ (that is a characteristic of each material) at which begins the formation of the crack; it means the disjunction of the parts. Using the same symbols of [26], in terms of power per volume unit, it is:

$$\Delta U\ f = \rho\, c\ \partial T / \partial t + E_i\, f \tag{3}$$

where $f$ is the test frequency (the number of load cycles per time unit), $\rho$ is the density of the material, $c$ is the specific heat of the material, $T$ is the temperature, in general a function of space and time, $E_i$ is the energy spent per cycle, which accrues as fatigue. Being in phase B, the temperature can be considered constant in the volume and time. In particular, in this phase, for a tract of specimen, distant from the edges (Fig. 2), the variation of temperature along the axis z of the specimen can be considered constant.

The heat $Q$ can be considered as the sum of the heat lost by conduction, by convention and radiation. So, in terms of thermal power, it is:

$$Q\ f\ A\, l = -\lambda\, \partial^2 T / \partial z^2\, A\, l + \alpha \left(T - T_a\right) p\, l + \kappa\, \sigma_n \left(T^4 - T_a^4\right) p\, l \tag{4}$$

where $A$ is area of specimen section (that is $b \cdot s$, where $b$ is the width of the specimen, $s$ is the thickness), $l$ is the vertical length of the considered portion of the specimen, $p$ is the perimeter of the section of the specimen, $T$ is the surface temperature of the specimen, $T_a$ is the ambient temperature, $\lambda$ is the coefficient of thermal conductivity, $\alpha$ is the coefficient of thermal exchange by convection, $\kappa$ is the surface emissivity, $\sigma_n$ is the Stephan-Boltzman constant.

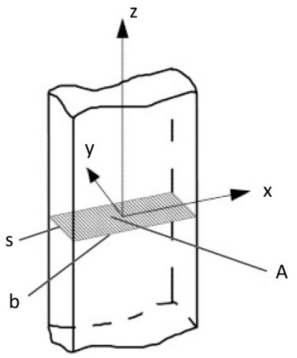


Fig. 2. A plain specimen with a rectangular cross section having area A [26].

When the temperature of the specimen is constant (as assumed for phase B) and the variations of the temperature are not higher than 80°, equation (4) becomes:

$$Q\, f = K\left(T - T_a\right) p / A \tag{5}$$

where $K$ is a coefficient which includes both the properties for convection and for irradiation [25].

Definitely, according to equations (1), (2), (3), it is:

$$W\ f = \oint \sigma\ d\varepsilon\ f = Q\ f + \rho\ c\ \partial T/\partial t + E_i\ f \tag{6}$$

and with the preceding assumptions, introducing equation (5), the power per volume unit can be written as:

$$\oint \sigma\ d\varepsilon\ f - E_i\ f = K\left(T - T_a\right) p/A \tag{7}$$

The first member of equation (7) allows to express $\beta_p$, the portion of supplied energy per volume unit transformed into heat during the phase B:

$$\beta_p = \frac{\oint \sigma\ d\varepsilon\ f - E_i\ f}{\oint \sigma\ d\varepsilon\ f} = \frac{K\left(T - T_a\right) p/A}{\oint \sigma\ d\varepsilon\ f} \tag{8}$$

If we indicate with $N_B$ the number of cycle corresponding to the crack formation (Fig. 1), we can write:

$$N_B \cdot E_i = E_l = \text{constant} \tag{9}$$

Therefore in all equations (3), (6), (7), (8), the term $E_i \cdot f$ can be expressed by $E_l \cdot f/N_B$.

The factor $\beta_p$ is also the part of the work related to the irreversible plastic deformations transformed into heat during the phase B of the diagram in Fig. 1, that is the relative damping (plastic) $\Psi = 8\varepsilon_p/\varepsilon_e$ ($\varepsilon_p$ is the plastic part of the deformation, $\varepsilon_e$ is the elastic deformation), which is only due to the perfect plastic deformations of the phase B, compared to the elastic energy per cycle:

$$\beta_p = \Psi = \frac{4E\ K\left(b + s\right)\left(T - T_a\right)}{bs\ f\ \sigma_m^2} \tag{10}$$

where $E$ is the Young's modulus, and $\sigma_m$ is the maximum amplitude of stress.

At the end of phase B in Fig. 1 the material has a first crack with a detachment of the surface that during phase C increases. The energy supplied from the outside allows the crack to grow until the size of the resistant section of the specimen cannot more resist and it breaks for crash [28-35].

Examining the surface temperature it is noticed (for steels) an increase continuous and almost linear with the number of cycles, and with a slope which is a function of the applied load, that is according a law of the type:

$$\Delta T = K_1\ \Delta T_s \left(\Delta N\right)^n \tag{11}$$

where $\Delta T_s$ is the stationary temperature increment of phase B, $K_1$ and $n$ are constants that depend on the characteristic of the material.

At the end of the specimen lifetime and after the formation of the crack (phase C), it can be assumed that the area of the crack $A_c$ grows following the same law of the temperature, until it reaches a value so that the resistant section will be lower than the ratio between the applied load and the tensile strength of the material:

$$A_c = K_2\ \Delta T \tag{12}$$

From equations (11) and (12) we obtain:

$$A_c = C_1 \, \Delta T_s \left(\Delta N\right)^n \qquad \text{with} \quad C_1 = K_1 \, K_2 \tag{13}$$

In the case of steels, as said before, the experience shows that, in the final phase, $n$ can assume the value of 1, which means that the temperature grows linearly with the number of cycles. Furthermore, in same case, the stationary temperature increment is related to the stress applied by the relation:

$$\Delta T_s = m \left(\sigma^2 - \sigma_o^2\right) \tag{14}$$

where the coefficient $m$ can be estimate as the slope of experimental lines (as will be show afterwards), $\sigma$ is the applied stress, and $\sigma_o$ is the fatigue limit. Therefore, according to equation (13) and (14), with $n = 1$, the area of the crack $A_c$ can be at last written as a function of the applied stress (in finite and differential forms):

$$A_c = C_1 \, m \left(\sigma^2 - \sigma_o^2\right) \Delta N \tag{15}$$

$$dA_c / dN = C_1 \, m \left(\sigma^2 - \sigma_o^2\right) \tag{16}$$

The constant $C_1$ can be determined after the breakage of the specimen. At this limit condition it is:

$$A_{c,r} = A - P / \sigma_u \tag{17}$$

where $A_{c,r}$ is the value of crack area at rupture point, $A$ is the original area of resistant section of the specimen, $P$ is the applied load and $\sigma_u$ is the tensile strength of the material. According to equation (15), $A_{c,r}$ is also:

$$A_{c,r} = C_1 \, m \left(\sigma_r{}^2 - \sigma_o^2\right) \Delta N_C \tag{18}$$

where $\sigma_r$ is the value of the stress of the last load step (stress to rupture), $\Delta N_C = N_R - N_B$ is the number of the cycles of the final part of diagram in Fig. 1 (phase C).

The constant $C_1$ can be determined by means of equations (17) and (18).

Finally we highlight the analogy between equation (16) and the classic Paris law:

$$da / dN = C \left(\Delta K\right)^n \qquad \text{with} \quad \Delta K = Y \, \Delta\sigma \sqrt{\pi \, a} \tag{19}$$

where $a$ is the crack length, $da/dN$ is the crack growth rate, $\Delta K$ is the range of the stress intensity factor, $C$ and $n$ are coefficients that depend on the material, $Y$ is a dimensionless parameter that depends on the geometry of the system, $\Delta\sigma$ is the range of cyclic stress amplitude.

## 3. Experimental tests and results

### *3.1. Materials and setup of the tests*

The tests have been performed on X5CrNi1810 steel specimens (Fig. 3), whit useful sizes $s$ = 5 mm, $b$ = 13 mm, $l$ = 60 mm (Fig. 2 and Fig. 3). The main mechanical properties of the materials are reported in Table 1.

Table 1. Mechanical properties of X5CrNi1810.

| Tensile strength [MPa] | Yield strength [MPa] | Young's modulus [MPa] | Elongation |
|---|---|---|---|
| 600 - 950 | 400 | 200000 | 25% |

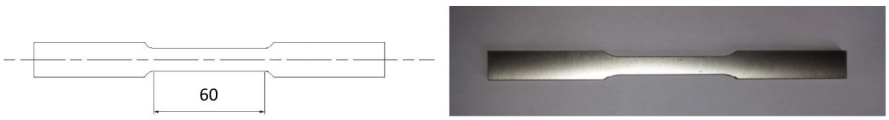


Fig. 3. Shape and size of the specimens.

Before each test, the specimens have been painted with a black opaque paint (RS Matt Black). The tests have been conducted using an electrohydraulic machine INSTRON 8501 with 100 kN maximum capacity. For the thermal sensing of the specimen surface temperature, the FLIR-3000 system has been used.

The loading ratio was $R = 0.1$ with a stepped trend such as that shown in Fig. 4, with load steps of 3000 cycles.

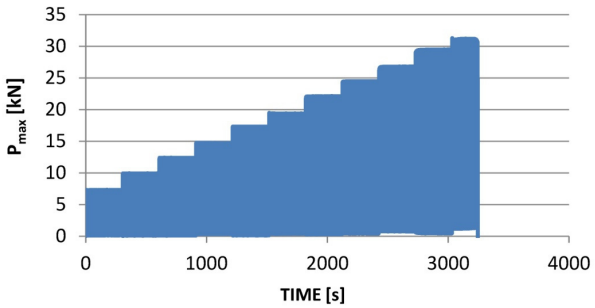


Fig. 4. Stepped trend of the applied loads.

The test frequency $f$ was equal to 10 Hz. During the test, the surface temperature was continually recorded. The recorded data were then analyzed in order to point out:

- the point (area) on the surface of the specimen with the higher temperature;
- the value of the stationary temperature $T_s$ in the phase B of diagram in Fig. 1, and then the stationary temperature increment $\Delta T_s$;
- the number of cycles $\Delta N_C = N_R - N_B$ with the fast increase in temperature (phase C in Fig. 1);
- the number of cycles $N_R$ which determines the break of the specimen;
- the temperature variation with the number of cycles in the phase C.

### *3.2. Results of the tests*

Proceeding as said before, it has been analyzed the temperatures during the test for each of the applied load. Fig. 5 shows the trend of temperature increment for the different applied load steps.

In Table 2 they have been reported the values of the stationary temperature increment, that result negligible for the first 3 steps. These are the values whom the temperature would have tended to, if it would has been adopted a higher number of step cycles, in this case defined at the end of the step (at the end of 3000 cycles of each step).

From Fig. 5 it has been also defined the number of cycles of the last load step (equal to 1700 cycles) which has caused an unexpected increase of the temperature. The value of $\Delta N_C$ is equal to 410 cycles and it refers to the sudden increase of the temperature $\Delta T_C$ of the last part of specimen life; it is equal to about 15 C°.

The diagram reported in Fig. 6 is obtained by means of the Risitano Method [7-13]: the x axis reports the square of maximum amplitude of the applied stress $\sigma_m$, the y axis reports the value of the thermal increment of the hotter point (areola) of the surface of the specimen.

It has been possible to identify the fatigue limit $\sigma_o$ equal to 268 MPa and the coefficient $m$ of the straight line interpolating the experimental data ($m = 0.00028$). The overall test results are: $\sigma_r = 500$ MPa stress value up to the

complete breakdown of the sample (last loading step); $\sigma_o$ = 268 MPa fatigue limit (resistance to the origin); $m$ = $2.8 \cdot 10^{-4}$ slope of the line $\Delta T_s$ - $\sigma_m^2$; $\Delta N_C$ = 410 number of cycles from the starting of the sudden increase in temperature to the breakage (cycles of the phase C in Fig. 1); $t$ = 0.037 slope of the temperature during the phase 3.

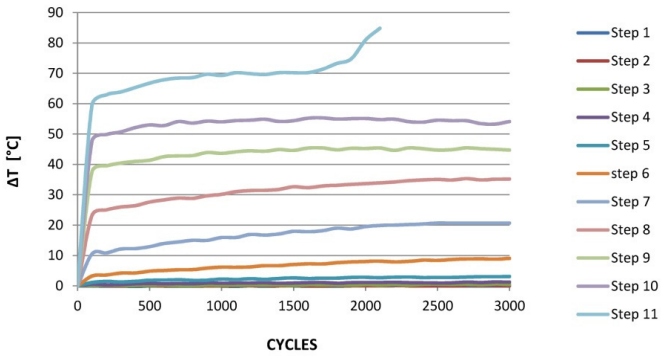


Fig. 5. Trends of the temperature increment.

Table 2. Load levels: specifications and stationary temperature increments.

| Load levels | Maximum stress $\sigma_m$ [MPa] | Elastic strain $\varepsilon_e$ | Stationary temp incr $\Delta T_s$ [°C] | $\beta_p = \Psi$ | N. of cycles at break $N_R$ | $\sigma^2 - \sigma_o^2$ [MPa$^2$] | $\Delta N_C$ |
|---|---|---|---|---|---|---|---|
| Step 1 | 115.38 | | 0.00 | | | | |
| Step 2 | 153.85 | | 0.08 | | | | |
| Step 3 | 192.31 | 0.00091 | 0.36 | | | | |
| Step 4 | 230.77 | 0.00110 | 1.07 | 0.069 | | | |
| Step 5 | 269.23 | 0.00128 | 2.81 | 0.132 | $2x10^6$ | | |
| Step 6 | 307.69 | 0.00146 | 8.97 | 0.327 | $72.00x10^3$ | $2.15x10^4$ | 3193 |
| Step 7 | 346.15 | 0.00165 | 21.21 | 0.616 | $30.50x10^3$ | $4.63x10^4$ | 1351 |
| Step 8 | 384.62 | 0.00183 | 35.11 | 0.817 | $18.40x10^3$ | $7.48x10^4$ | 816 |
| Step 9 | 423.08 | 0.00201 | 45.05 | 0.873 | $14.24x10^3$ | $10.55x10^4$ | 635 |
| Step 10 | 461.54 | 0.00220 | 54.38 | 0.886 | $11.88x10^3$ | $13.91x10^4$ | 526 |
| Step 11 | 500.00 | 0.00238 | 69.69 | 0.968 | $9.27x10^3$ | $17.66x10^4$ | 410 |

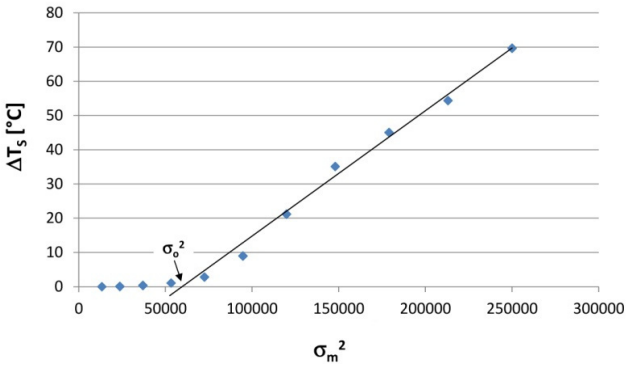


Fig. 6. Trend of the stationary temperature increment as a function of the square of maximum stress amplitude.

The above analysis has been repeated on 3 different specimens and the trends of the variation of the surface temperature were very similar with a difference of not over than the 3%. In the Fig. 7a and Fig. 7b they have been reported the diagrams of the surface temperature increment of the other two specimens with varying the load (parameter of the curves) and the number of cycles. They show the sudden increase of the temperature in proximity to breakage (at the last loading step). They are very similar to diagram related to the specimen 1 (Fig. 5). Proceeding as for the specimen 1, it has been defined the data reported in Table 3 for all the specimens.

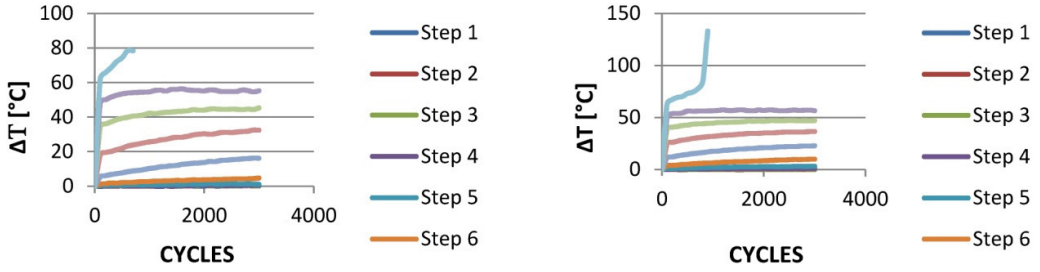


Fig. 7. Increment of surface temperature: a) specimen2; b) specimen 3.

Table 3. Trial results for each specimen.

| Specimen | Stress to rupture $\sigma_r$ [MPa] | Fatigue limit $\sigma_o$ [MPa] | Slope $\Delta T_s$-$\sigma_m^2$ m | N. of cycles (phase C) $\Delta N_C$ | Slope T (phase C) t | $\Phi$ | $\Phi_{cr}$ | $\Phi_{cr}/\Phi$ |
|---|---|---|---|---|---|---|---|---|
| 1 | 500 | 268 | 0.00028 | 410 | 0.037 | $645.81 \times 10^3$ | $33.57 \times 10^3$ | 0.052 |
| 2 | 500 | 272 | 0.00026 | 490 | 0.029 | $516.60 \times 10^3$ | $35.50 \times 10^3$ | 0.069 |
| 3 | 500 | 269 | 0.00027 | 400 | 0.172 | $618.80 \times 10^3$ | $38.70 \times 10^3$ | 0.062 |

### *3.3. Analysis of the results*

From the data obtained by the maps of temperature it can be built some tables, as Table 2 ,where for each of the loading step it has been determined the value $\beta_p$ expressed by equation (10), that is the internal damping in phase B. The thermal increase of the specimen surface - concerning the last loading step - is equal to 69.69 ° C.

Using equations (17) and (18) it has been determined the value of $C_1$, which is equal to $2.06 \cdot 10^{-4}$, and from equation (13) the values of $\Delta N_C$ reported in the Table 2. These values represent the number of cycles of the last part of lifetime of the specimen. Table 2 still refers to the specimen 1. For reasons of space, the tables related to the specimens 2 and 3 have not been reported, but they almost correspond with that of the specimen1.

Fig. 8 shows the trend of the factor $\beta_p$, that according to (10) expresses the internal damping also, during the phase B as a function of the elastic strain $\varepsilon_e$ (Table 2). In Table 3, for the three tested specimens, it has been reported the parameter $\Phi = \Delta T \cdot N_R$, that is proportional to the amount of the heat exchanged with the outside throughout the test, less than the overall exchange coefficient $K$ and the exchange surface of the specimen. The heat exchanged, in it turn, is proportional to the energy limit at break $E_l$ [13]. The second-last column of the Table 2 show the values related to the fatigue curve (Wöhler curve) of Fig. 8, obtained as it has been thoroughly described in [13], starting from the hypothesis, validated in literature, that the energy necessary to cause the breakage of the material (component) is a constant of the material itself. The energetic parameter $\Phi$ allows to go back up (knowing the temperature and the applied strain) to the number of cycles of the residual life of the specimen. This parameter $\Phi$ calculated for the three specimens has been reported in Table 3. In the second-last column of the same table it has been reported $\Phi_{cr}$, that is the share of $\Phi$ proportional to the energy used to break the specimen after the crack formation. This share is constant. The values of the ratio between the two quantities $\Phi_{cr}/\Phi$ show that the energy share necessary to cause the complete break of the specimen, after the crack formation, is very small (less than 7%)

in comparison to the breakage energy limit, and substantially constant. Finally, the equations (11), (12), (13) allow to calculate also the increase of the temperature during the last phase for the different values of the applied stress.

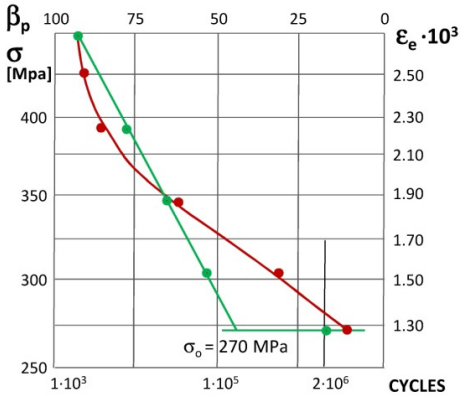


Fig. 8. Wöhler curve at R = 0.1 and f = 10 Hz (in green), and factor $\beta_p$ (in red) for the X5CrNi1810 steel.

## 4. Conclusions

The thermographic technique has been applied to the specimens of X5CrNi1810 steel in order to evaluate: the relative damping during the plastic phase; the beginning of the crack formation during the fatigue tests; how the crack advances.

Although the results need further confirmation, they are consistent with the results found in the past years by operating on various steels and they have never been analyzed from the point of view assumed in the present work. These results can be summarized as follows:

- the plastic energy can be converted into heat during the plastic deformation phase;
- from the beginning of the test, the point can be determined where the process of the local microplasticization starts; it coincides with the point where it arises the microcrack which will increase up to the breakage;
- it is possible to define the number of cycles which determine the crack beginning, and also the one at which the complete rupture takes place; the first one is detectable by the sudden increase of the temperature, which gets on almost linearly until failure;
- it is possible to estimate the increase of the crack area.

The knowledge of the residual life, related to the phase of crack beginning and progress of its amplitude (a few hundreds of cycles), recognizable by means of the sudden change in temperature (up to that moment constant), can be used to prepare immediately maintenance operations.

The authors intend to continue this research analyzing other available data, but using the same point of view assumed for this work.

## References

[1] R. Giovannozzi, Costruzione di Macchine, Vol. 1, second ed. Patron, Bologna, 1965.
[2] G.I. Taylor, H. Haring, The latent energy remaining in metal after cold working, Proc. R. Soc. A 134 (1934) 307–326.
[3] D. Dengel, H. Harig, Estimation of the fatigue limit by progressively-increasing load tests, Fatigue Fract. Eng. Mater. Struct. 3 (1980) 113–128.
[4] P.D. Stanley, W.K. Chan, Quantitative stress analysis by means of the thermoelastic effect, J. Strain Analysis 20 (1985) 129-137.
[5] T. Caltabiano, A. Geraci, M. Orlando, Thermal infrared analysis of specimens under fatigue loading (in italian), Il Progettista Industriale 2 (1984) 66-69.
[6] G. Curti, G. La Rosa, M. Orlando, A. Risitano, Analisi tramite infrarosso termico della ‘temperatura limite’ in prove di fatica, XIV Convegno Nazionale AIAS, Catania, 1986.

[7] G. Curti, A. Geraci, A. Risitano (1989) A new method for rapid determination of the fatigue limit (in italian), Ingegneria Automotoristica 42 (1989) 634–636.
[8] A. Geraci, G. La Rosa, A. Risitano, Influence of frequency and cumulative damage on the determination of fatigue limit of materials using the thermal infrared methodology, Proceedings of the 15th Polish National Symposium on Experimental Mechanics of Solids, Warsaw, 1992, pp. 63-65.
[9] A. Geraci, G. La Rosa, A. Risitano, M. Grech, Determination of the fatigue limit of an austempered ductile iron using thermal infrared imagery, SPIE International Conference, St. Petersburg, 1995.
[10] G. Fargione, A. Geraci, G. La Rosa, A. Risitano, M. Grech, Determinazione del limite di fatica in materiali sottoposti a differenti trattamenti termici mediante considerazioni energetiche, XXVI Convegno Nazionale AIAS, Catania, 1997
[11] G. Fargione, A. Geraci, G. La Rosa, A. Risitano, Determinazione rapida della curva di fatica con metodo termografico, XXVII Convegno Nazionale AIAS, Perugia, 1998.
[12] G. La Rosa, A. Risitano, Thermographic methodology for rapid determination of the fatigue limit of materials and mechanical components, Int. J. Fatigue 22 (2000) 65–73.
[13] G. Fargione, A. Geraci, G. La Rosa, A. Risitano, Rapid determination of the fatigue curve by the thermographic method, Int. J. Fatigue 24 (2002) 11–19.
[14] M.P. Luong, Infrared thermographic scanning of fatigue in metals, Nuc. Eng. Des. 158 (1995) 363–376.
[15] A. Fatemi, L. Vangt, Cumulative fatigue damage and life prediction theories: a survey of the state of the art for homogeneous materials, Int. J. Fatigue 20 (1998) 9–34.
[16] F. Curà, G. Curti, R. Sesana, A new iteration method for the thermographic determination of fatigue limit in steels, Int. J. Fatigue 27 (2005) 453–459.
[17] P. Starke, F. Walther, D. Eifler, PHYBAL: a new method for lifetime prediction based on strain, temperature and electrical measurements, Int. J. Fatigue 28 (2006) 1028–1036.
[18] M. Amiri, M.M. Khonsari, Rapid determination of fatigue failure based on temperature evolution fully reversed bending load, Int. J. Fatigue 32 (2010) 382–389.
[19] C. Clienti, G. Fargione, G. La Rosa, A. Risitano, G. Risitano, A first approach to the analysis of fatigue parameters by thermal variations in static tests on plastics, Engineering Fracture Mechanics 77 (2010) 2158-2167.
[20] A. Risitano, Mechanical Design, CRC Press, New York, 2011.
[21] G. Fargione, D. Tringal3, E. Guglielmino, G. Risitano, Fatigue characterization of mechanical components in service, Frattura ed Integrità Strutturale 26 (2013) 143-155.
[22] A. Risitano, G. Risitano, Determining fatigue limits with thermal analysis of static traction tests, Fatigue Fract. Eng. Mater. Struct. 36 (2013) 631-639
[23] V. Crupi, G. Epasto, E. Guglielmino, G. Risitano, Thermographic method for very high cycle fatigue design in transportation engineering, P. I. Mech. Eng. C – J. Mech., Special Issue "Fatigue Design and Analysis in Transportation Engineering", published online 2014.
[24] F. Maquin ,F. Pierron, Heat dissipation measurements in low stress cyclic loading of metallic materials: from internal friction to micro-plasticity, Mechanics of Materials 41 (2009) 928–942.
[25] G. Fargione, A. Geraci, L. Maiolino, A. Risitano, Influenza della storia di carico sull'energia limite a rottura per materiali ad elevato rilascio termico, XXX Convegno Nazionale AIAS, Alghero (SS), 2001.
[26] G. Meneghetti, Analysis of the fatigue strength of a stainless steel based on the energy dissipation, Int. J. Fatigue 29 (2007) 81-94.
[27] O.A. Plekhov, T. Pain-Luc, N. Saintier, S. Uvarov, O. Naimark, Theoretical analysis, infrared and structural investigations of energy dissipation in metals under cyclic loading, Mater. Sci. Eng. A 462 (2007) 367-369.
[28] C.E. Feltner, J.D. Morrow, Microplastic strain hysteresis energy as a criterion for fatigue fracture, Trans. ASME, Series D, J. Basic Eng. 83 (1961) 15–22.
[29] E.H. Jordan, Notch-root plastic response by temperature measurement, Exp. Mech. 25, (1985) 24–31.
[30] J.L. Chaboche, Continuum damage mechanics: part I - general concepts, Trans. ASME, Series T, J. Appl. Mech. 55 (1988) 59–64.
[31] A. Carpinteri, Meccanica dei Materiali e della Frattura, Pitagora Editore, Bologna, 1992.
[32] P. Lazzarin, R. Zambardi, The equivalent strain energy density approach reformulated and applied to sharp V-shaped notches under localised and generalised plasticity, Fatigue Fract. Eng. Mater. Struct. 25 (2002) 917–928.
[33] B. Atzori, P. Lazzarin, G. Meneghetti, Fracture mechanics and notch sensitivity, Fatigue Fract. Eng. Mater. Struct. 26 (2003) 257–267.
[34] L. Susmel, N. Petrone, Multiaxial fatigue life estimations for 6082-T6 cylindrical specimens under in-phase and out-of-phase biaxial loadings, in: A. Carpinteri, M. de Freitas, A. Spagnoli (Eds.), Biaxial/Multiaxial Fatigue and Fracture, Elsevier, Oxford, 2003, pp. 83–104.
[35] M. Ohata, T. Fukahori, F. Minami, Damage model for predicting the effect of steel properties on ductile crack growth resistance, Int. J. Damage Mech. 19 (2010) 441–459.